# Statistical mechanical analysis of linear programming relaxation for combinatorial optimization problems

Satoshi Takabe* and Koji Hukushima

*Graduate School of Arts and Sciences, The University of Tokyo, 3-8-1 Komaba, Meguro-ku, Tokyo 153-8902, Japan*

(Received 28 January 2016; revised manuscript received 13 April 2016; published 26 May 2016)

Typical behavior of the linear programming (LP) problem is studied as a relaxation of the minimum vertex cover (min-VC), a type of integer programming (IP) problem. A lattice-gas model on the Erdös-Rényi random graphs of $\alpha$-uniform hyperedges is proposed to express both the LP and IP problems of the min-VC in the common statistical mechanical model with a one-parameter family. Statistical mechanical analyses reveal for $\alpha = 2$ that the LP optimal solution is typically equal to that given by the IP below the critical average degree $c = e$ in the thermodynamic limit. The critical threshold for good accuracy of the relaxation extends the mathematical result $c = 1$ and coincides with the replica symmetry-breaking threshold of the IP. The LP relaxation for the minimum hitting sets with $\alpha \geqslant 3$, minimum vertex covers on $\alpha$-uniform random graphs, is also studied. Analytic and numerical results strongly suggest that the LP relaxation fails to estimate optimal values above the critical average degree $c = e/(\alpha - 1)$ where the replica symmetry is broken.

DOI: 10.1103/PhysRevE.93.053308

## I. INTRODUCTION

Relaxation for discrete optimization problems is a basic and generic strategy to solve them approximately. Using relaxation techniques by which a part of an optimization problem is modified, we substitute easy problems for hard problems to solve. A striking example is a relaxation for integer programming (IP) problems. Although the IP problem is generally NP hard, the relaxed linear programming (LP) problem belongs to the class of P [1]. This fact demonstrates that the LP relaxation enables us to approximate the IP problem in polynomial time. The technique is applied to various practical optimizations such as vehicle routing [2], scheduling [3], and Boolean compressed sensing [4].

In this relaxation strategy, evaluating the performance of approximations is an important issue both for worst-case and average-case analysis. With improvement of mathematical techniques, worst-case analyses have been strongly advanced in theoretical computer science. The relaxation plays a key role in the construction of constant-factor-approximation algorithms for combinatorial optimization problems [5]. Another attractive issue is average-case behavior of approximations for randomized optimization problems. It provides not only prediction of the performance of approximations but also typical hardness of optimizations. Analytical studies of greedy algorithms reveal average properties of problems and their intrinsic structures [6]. It is still challenging, however, to study the typical behavior of relaxation analytically.

Typical hardness of the optimization problems also has attracted physicists' interests because it is described using a type of phase transition in statistical mechanics. With the development of the spin-glass theory since the 1970s [7], a mean-field picture with replica theory has been established. The spin-glass techniques were then applied to many optimization problems. The picture of phase transitions breaking a replica symmetry (RS) is associated with the typical hardness of optimizations [8,9].

Among them, the minimum vertex cover (min-VC) has also been studied as a good example to which the spin-glass theory is applied. It is a well-known NP-hard combinatorial optimization problem defined on a graph. Various types of exact or approximation algorithms such as a leaf removal (LR) [10] are proposed. The difficulty of approximation has been studied by computer scientists [11]. In the statistical mechanical view, the average-case properties have been studied extensively in terms of phase transition [12]. For instance, mean-field analyses of the min-VC on random graphs conclude that replica symmetry breaking (RSB) occurs at a critical average degree [13–15]. Typical behavior of the LR and its variants are also studied in solving the min-VC approximately [16,17]. They strongly associate the typical hardness in approximation with the mean-field picture of the RSB transition. Recently, average properties of the minimum hitting set (min-HS), the min-VC on hypergraphs, are also analyzed [18,19]. While the min-HS involves the multibody interactions from the view of statistical mechanics, it is suggested that the goodness of the LR algorithm is characterized by the phase transition in the spin-glass theory.

The nontrivial relation between the replica symmetry and the typical hardness in approximation was also suggested in the case of continuous relaxation by physicists in [20,21]. They studied continuous relaxation with a spherical constraint, which changes optimization problems to NP-hard quadratically constrained programming problems. Although it is still difficult to solve the relaxed problems, these studies indicate the existence of the typical tightness of relaxation techniques. It is of interest whether the relation holds in the case of polynomially solvable relaxation such as the LP relaxation. In theoretical computer science, mathematical analysis of the LP relaxation for min-VCs with weights following an exponential distribution is performed [22]. Such analyses revealed that the LP relaxation is closely related to the belief propagation in statistical physics and it is asymptotically tight if the belief propagation can converge with high probability. Recently, the typical behavior of the LP relaxation for the unweighted min-VCs is studied numerically [23], suggesting that a threshold of good-wrong approximation is close to the RS-RSB one and

*s_takabe@huku.c.u-tokyo.ac.jp

 

that it is well above a mathematical prediction. In our previous paper [24], we proposed a statistical mechanical analysis of the LP relaxation and showed that these two thresholds are coincident. These results constitute a demonstration that the LP relaxation typically approximates an NP-hard problem with good accuracy.

As described in this paper, we study the typical behavior of the LP relaxation for the min-VCs defined on $\alpha$-uniform hypergraphs using statistical mechanical techniques. The min-VC with $\alpha = 2$ has a novel property called half integrality, which enables us to reduce the continuous degree of freedom in the LP to three states. Consequently, a three-state lattice-gas model called an LP-IP model is introduced for studying the LP relaxation of the min-VC. Statistical mechanical analysis derives successfully an analytical threshold of the typical hardness of the LP relaxation, which coincides with the RS-RSB transition of the original min-VC. Although a brief report on the LP-IP model based on the replica method has already been published [24], this paper presents the full details of statistical mechanical analyses of the LP relaxation for min-VCs including the analysis of the cavity method. Additionally, we discuss the LP relaxation for the min-HS to examine whether its typical hardness is associated with the RS-RSB transition. Because the min-HS, unfortunately, has no half integrality, the LP-IP model does not completely capture the LP relaxation of the min-HS but still provides an interesting feature on the stability of integral solutions against a perturbation toward continuous values.

This paper is organized as follows. In the following section, we define the min-VC and its LP relaxation. To investigate randomized problems, random graphs and their useful properties are also introduced. We explain the definition of average-case properties over random graphs and the typical behavior of the LP relaxation. In Sec. III we propose the LP-IP model and present details of the analysis using the replica method. The model with three-state Ising spins includes the min-VC. It also includes LP-relaxed solutions as specific limits in a model parameter. By choosing the parameter in the model appropriately, we obtain three RS solutions for ground states of the model. We also devote some discussion to their stability. In Sec. IV, we present some numerical results of the LP relaxation. In the case of the min-VCs, the statistical mechanical analysis agrees well with the numerical results. For the min-HS, however, analytical results are no longer coincident with the numerical results but these results suggest that the typical hardness of the LP relaxation is associated with the RS-RSB transition. The last section is devoted to a summary and discussion of the results and salient implications. In the Appendix, an alternative cavity analysis of the LP-IP model is presented.

## II. MIN-VC, LP RELAXATION, AND THEIR RANDOMIZATION

### A. Definitions of min-VC and hypergraphs

Let an $\alpha$-uniform hypergraph $G = (V, E)$ be a hypergraph of which the edges connect to $\alpha$ different vertices in $V$ without multiplicity. Each vertex is labeled by $i \in V = \{1, \cdots, N\}$. Each edge in $G$ is then defined as $E_a = (i_1, \cdots, i_\alpha) \in E \subset V^\alpha$ $(i_1 < \cdots < i_\alpha)$, where $a \in \{1, \cdots, M = |E|\}$. We assign a binary variable $x_i$ to the $i$th vertex. The vertex $i$ is called covered if $x_i = 1$, and is called uncovered otherwise.

The min-VC problem offers each edge for the constraint that it should connect to at least one covered vertex. The covered vertex set $V'$ is defined as a subset of $V$ that satisfies all constraints for edges. The (unweighted) min-VC problem searches for the minimum cardinality $|V'|$ of the covered vertex set. As described in this paper, the minimum cover ratio $x_c(G) = |V'|/N$ on $G$ is studied especially in the large-$N$ limit. Then, it is expressed as a form of the IP problem as

$$\begin{aligned} &\text{Minimize} \quad x_c^{\mathrm{IP}}(G) = N^{-1}\boldsymbol{c}^{\mathrm{T}}\boldsymbol{x}, \\ &\text{Subject to} \quad A\boldsymbol{x} \geqslant \mathbf{1}, \boldsymbol{x} \geqslant \mathbf{0}, \boldsymbol{x} \in \mathbb{Z}^N, \end{aligned} \tag{1}$$

where $\boldsymbol{x} = (x_1, \cdots, x_N)^{\mathrm{T}}$, $\boldsymbol{c} = (1, \cdots, 1)^{\mathrm{T}}$, and an $M \times N$ incident matrix $A = (a_{ij})$ is defined as $a_{ai_1} = \cdots = a_{ai_\alpha} = 1$ if $(i_1, \cdots, i_\alpha) = E_a$ and $a_{aj} = 0$ otherwise. The inequality holds on each element of vectors. Here, the min-VC problem on hypergraphs ($\alpha \geqslant 3$) is especially called the min-HS. The min-VC and min-HS, as well as other IP problems, are difficult to solve exactly in their worst case.

### B. LP relaxation

The LP relaxation is a fundamental approximation for the IP problem. To use the LP relaxation, it is sufficient to replace the integral conditions $\boldsymbol{x} \in \mathbb{Z}^N$ in the IP with continuous ones $\boldsymbol{x} \in \mathbb{R}^N$. In the case of the min-VC, the LP-relaxed problem reads

$$\begin{aligned} &\text{Minimize} \quad x_c^{\mathrm{LP}}(G) = N^{-1}\boldsymbol{c}^{\mathrm{T}}\boldsymbol{x}, \\ &\text{Subject to} \quad A\boldsymbol{x} \geqslant \mathbf{1}, \boldsymbol{x} \geqslant \mathbf{0}, \boldsymbol{x} \in \mathbb{R}^N. \end{aligned} \tag{2}$$

Although this change on degrees of freedom engenders good feasibility of the problems, it might provide optimal solutions different from the IP problems.

From the view of computational complexity and approximation, it is important whether the optimums can be obtained exactly, or not, using the LP relaxation. The Hoffman-Kruskal theorem is a mathematical result for the LP relaxation [25]. Let us consider an LP problem given as $\min \tilde{\boldsymbol{c}}^{\mathrm{T}}\boldsymbol{x}$, s.t. $B\boldsymbol{x} \geqslant \boldsymbol{p}$ in general. We define a matrix $B$ as a totally unimodular matrix if all sub-determinants of $B$ take only $-1$, 0, or 1. The theorem claims that the optimal value of the LP-relaxed problem is equal to that of the original IP problem if the matrix $B$ is a totally unimodular matrix and $\boldsymbol{p}$ is an integral vector. Because an incident matrix $A$ of a hypertree, i.e., a hypergraph with no cycles, is totally unimodular, the theorem ensures that the optimal value of the min-VC on a hypertree can be found exactly by the LP relaxation.

### C. Randomized min-VC

As described in Sec. I, it is our goal to find a phase transition of the typical behavior of the LP relaxation for the randomized min-VC. Here, we introduce the Erdös-Rényi random graphs as a graph ensemble. The Erdös-Rényi random graphs are generated by choosing edges from all pairs of $N$ vertices with probability $p$. The number of edges is then expected to be $pN(N-1)/2$. The average degree defined by the average

number of edges connected to each vertex is $p(N-1)$. In this paper, we set $p = c/N$ where $c$ is a constant average degree of $O(1)$, leading to a sparse random graph. In the case of $\alpha$-uniform hypergraphs, the definition of the ensemble is similar to the $\alpha = 2$ case. Each edge is set randomly with probability $c(\alpha-1)!/N^{\alpha-1}$ from every $\alpha$-tuple of vertices. The degree distribution then converges to the Poisson distribution with mean $c$ in the large $N$ limit. One of the novel properties of the ensemble is to exhibit a bond-percolation transition at $c_p = 1/(\alpha-1)$. If $c < c_p$, most of vertices belong to trees and a finite number of short cycles exist. Otherwise, a giant connected component emerges. There exists a huge number of long cycles in the component. Another property is called locally tree-like structure [26]. The likelihood of short cycles decays as the size of graphs grows if the average degree $c$ is constant. The absence of short cycles indicates that a state on a vertex is predictable using information related to its neighbors. This structure is especially important when the cavity method is applied to a system.

The min-VC problems on the Erdös-Rényi random graphs have been studied using the replica method [13] and cavity method [14,27] developed in the spin-glass theory. These studies provide an estimation of the average minimum-cover ratio, i.e., an optimal value averaged over random graphs in the thermodynamic limit, defined as

$$x_c^{\mathrm{IP}}(c) = \lim_{N\to\infty} \overline{x_c^{\mathrm{IP}}(G)}, \tag{3}$$

where $\overline{(\cdots)}$ is an average over the Erdös-Rényi random graphs with $N$ vertices and the average degree $c$. These statistical mechanical analyses under the RS ansatz estimate $x_c(c)$ of the problem, including the case of hypergraphs, for $c < c^* = e/(\alpha-1)$ ($e = 2.71\cdots$) [18]. Above the threshold $c^*$, the replica symmetry is broken, which results in an incorrect estimation of the minimum-cover ratio. Aside from these studies, it was also confirmed that a polynomial-time approximation algorithm called leaf removal works well in the RS region [16]. However, in the RSB region, this graph-removal algorithm cannot estimate $x_c$ correctly. A giant connected component called the LR core is left. These results suggest that the replica symmetry in the spin-glass theory has a close relation to the typical behavior of an approximation algorithm [18,19].

Here, we specifically examine the LP relaxation for min-VCs and min-HSs. The LP-relaxed average minimum-cover ratio $x_c^{\mathrm{LP}}(c)$ is also a valid quantity used to evaluate the typical behavior of the LP relaxation. Given that the average degree $c < c_p$, a large part of the graphs consists of (hyper)trees. The connected component with short cycles consists of $O(\log N)$ vertices. Therefore, it does not affect the average ratio. From the Hoffman-Kruskal theorem, the LP-relaxed optimal value on (hyper)trees is equal to that of the original min-VC problems. We therefore confirm that $x_c^{\mathrm{LP}}(c) = x_c^{\mathrm{IP}}(c)$ if $c < c_p$.

Once the bond percolation occurs above $c_p$, the Hoffman-Kruskal theorem cannot be applied directly because a giant component with long cycles exists. The recent numerical study suggests that the relation $x_c^{\mathrm{LP}}(c) = x_c^{\mathrm{IP}}(c)$ is correct up to $c = 2.62(17)$ [23] above the bond-percolation threshold $c_p = 1$ in the case of min-VCs with $\alpha = 2$. In the next section, we analytically obtain the threshold by analyzing the LP-IP model.

## III. LP-IP MODEL

In this section, typical behavior of the LP relaxation for min-VC problems is studied using the replica method. Although it is difficult in general to analyze a model with continuous spin variables on sparse random graphs, a novel property called half integrality enables us to estimate the LP-relaxed min-VC with $\alpha = 2$ using a statistical mechanical method.

### A. Half integrality

By applying an appropriate transformation, the LP problem is able to map onto an optimization problem constrained on a convex polytope or simplex. Then, an extreme-point solution is defined with a feasible solution located on an extreme point of the polytope. It is sufficient to search an extreme-point solution for solving the LP problem the cost function of which is linear. The simplex method, the first useful algorithm for the LP problems, is based on this strategy [28]. Although it takes exponential time in the worst case, it solves most of the problems in polynomial time.

In the case in which $\alpha = 2$, the LP-relaxed min-VC problems have half integrality, that is, all elements of an arbitrary extreme-point solution consist of half integers [29]. From this property, we define the minimum half-integral ratio,

$$p_h(G) = \frac{1}{N} \min_{\boldsymbol{x}:\,\text{optimal}} \left| \left\{ i \in V \,\middle|\, x_i = \frac{1}{2} \right\} \right|, \tag{4}$$

on a graph $G$. It results in $x_c^{\mathrm{LP}}(G) = x_c^{\mathrm{IP}}(G)$ if $p_h(G) = 0$. Considering random graphs, the average ratio of half integers is defined as

$$p_h(c) = \lim_{N\to\infty} \overline{p_h(G)}. \tag{5}$$

Along with $x_c^{\mathrm{LP}}(c)$, $p_h(c)$ provides a good evaluation of the typical behavior of the LP relaxation. The half integrality also enables us to analyze the LP relaxation by the three-state Ising model with hard-core constraints as shown later. As described in this paper, we specifically study the model by the replica method or cavity method. However, the LP relaxation for the min-HS ($\alpha \geqslant 3$) has no half integrality. One can expect that variables in the LP-relaxed solutions take multiples of $1/\alpha$, but this is not the case. Figure 1 presents a frequency distribution of variables of the LP-relaxed solutions solved by a revised simplex method using LP_solve_5.5 solver [30], which searches extreme-point solutions. A discrete property of the solutions for $\alpha > 2$ is denied by the observation. In this case, we discuss the results of the model as an approximation of the LP relaxation and examine its validity mainly using numerical simulations.

### B. LP-IP model

The min-VC and min-HS are represented by a hard-core lattice-gas model. We first transform an occupancy variable $x_i$ to a three-state Ising variable $\sigma_i \in \{-1,0,1\}$ by $\sigma_i = 2x_i - 1$. If $\sigma_i = 1$, vertex $i$ is covered and $\sigma_i = 0$ represents $x_i = 1/2$. The partition function of the three-state Ising model is the

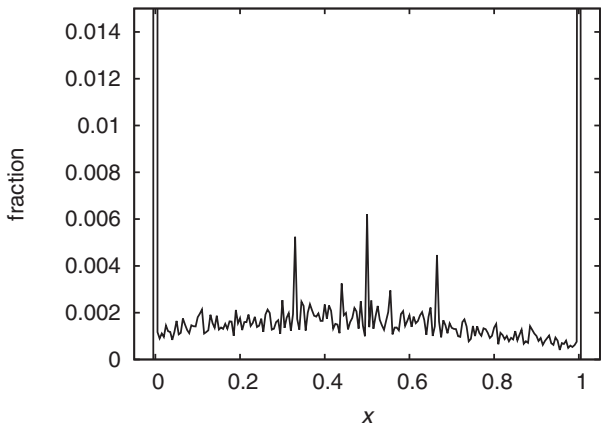


FIG. 1. Frequency distribution of variables in the LP-relaxed min-HS, averaged over 100 random graphs with $\alpha = 3$, $N = 1600$, and $c = 2.0$.

following:

$$\Xi(G)=\sum_{\boldsymbol{\sigma}}\exp\left(-\mu\sum_{i}\sigma_i\right)\prod_{\{i_1,\cdots,i_\alpha\}\in E}\theta\left(\sum_{j=i_1}^{i_\alpha}\sigma_j+\alpha-2\right). \tag{6}$$

Therein, $\theta(x)$ is a unit step function that takes one if $x \geqslant 0$ and zero otherwise. Although the ground-state energy corresponds to the LP relaxed value, the ground states of the model might differ from the optimal extreme-point solutions. On graph $G_1 = (\{1,2\},\{(1,2)\})$, for example, optimal extreme-point solutions are $(x_1,x_2) = (1,0)$ and $(0,1)$, but the ground states of the model (6) include another solution $(x_1,x_2) = (1/2,1/2)$ in addition to the correct ones, which produces a wrong estimation of $p_h(G_1)$. Omitting this trivial ground state, a penalty term is introduced as follows:

$$\Xi_r(G) = \sum_{\boldsymbol{\sigma}}\exp\left(-\mu\sum_i\sigma_i-\mu^r\sum_i\left(1-\sigma_i^2\right)\right)\times\prod_{\{i_1,\cdots,i_\alpha\}\in E}\theta\left(\sum_{j=i_1}^{i_\alpha}\sigma_j+\alpha-2\right). \tag{7}$$

The penalty term adds some cost with a constant $r \in \mathbb{R}$ to half-integral variables. When $r$ is larger than 1, it is regarded as Ising spin constraints in the large-$\mu$ limit. Consequently, the ground states correspond to IP optimal solutions. This limit is defined as an IP limit. In the case in which $0 < r < 1$ and $\mu \to \infty$, the number of half integers is minimized by the penalty term though the ground-state energy is equivalent to LP-relaxed optimal values. We thus call this limit an LP limit. For negative $r$, the penalty terms have no influence on the system. This three-state limit provides the same ground states obtained by Eq. (6), including trivial ground states. We designate this effective model the LP-IP model, which enables us to estimate the LP relaxation and original IP problems in the case in which $\alpha = 2$ by setting the value of $r$ appropriately.

The average minimum cover ratios, $x_c^{\mathrm{LP}}(c)$ and $x_c^{\mathrm{IP}}(c)$, are the densities averaged over the random graph ensemble. It is our task to calculate an average free-energy density $N^{-1}\overline{\ln \Xi_r(G)}$. The replica method and cavity method are often used to estimate the free-energy density directly. Here, we use the replica method developed in an earlier study [31]. The alternative cavity method is presented in the Appendix, where the essentially same results derived in this section are obtained.

In the replica method, we use the replica trick $\overline{\ln \Xi_r(G)} = \lim_{n\to 0}(\overline{\Xi_r(G)^n}-1)/n$. Considering that each edge is set randomly with probability $(\alpha-1)!c/N^{\alpha-1}$, the average over random graphs is taken as shown below:

$$\begin{aligned}\overline{\Xi_r(G)^n} &= \sum_{\boldsymbol{\sigma}}\exp\left(-\mu\sum_{a=1}^{n}\sum_i\sigma_i^a-\mu^r\sum_{a=1}^{n}\sum_i\left\{1-\left(\sigma_i^a\right)^2\right\}\right)\overline{\prod_{a=1}^{n}\prod_{\{i_1,\cdots,i_\alpha\}\in E}\theta\left(\sum_{j=i_1}^{i_\alpha}\sigma_j+\alpha-2\right)}\\ &= \sum_{\boldsymbol{\sigma}}\exp\left[-\mu\sum_{a,i}\sigma_i^a-\mu^r\sum_{a,i}\left\{1-\left(\sigma_i^a\right)^2\right\}-\frac{cN}{\alpha}+\frac{c}{\alpha N^{\alpha-1}}\prod_{i_1<\cdots<i_\alpha}\prod_{a=1}^{n}\theta\left(\xi^a+\sum_k\xi_k^a+\alpha-2\right)+O(1)\right].\end{aligned} \tag{8}$$

We introduce an order parameter of the replicated system [31] as

$$c(\vec{\xi}\,) = \frac{1}{N}\sum_i\prod_{a=1}^{n}\delta\left(\xi^a,\sigma_i^a\right), \tag{9}$$

where $\delta(\cdot,\cdot)$ is Kronecker's delta. Rewriting Eq. (8) by using a replicated vector $\vec{\xi}$ and its frequency ratio, the partition function is

$$\begin{aligned}\overline{\Xi_r(G)^n} \simeq \int_\Lambda\left(\prod_{\vec{\xi}}dc(\vec{\xi}\,)\right)\exp\left\{N\left[-\sum_{\vec{\xi}}c(\vec{\xi}\,)\ln c(\vec{\xi}\,)-\mu\sum_{\vec{\xi}}c(\vec{\xi}\,)\xi-\mu^r\left(n-\sum_{\vec{\xi}}c(\vec{\xi}\,)\tilde{\xi}\right)-\frac{c}{\alpha}\right.\right.\\ \left.\left.+\frac{c}{\alpha}\sum_{\vec{\xi},\{\vec{\xi}_k\}}c(\vec{\xi}\,)\prod_{k=1}^{\alpha-1}c(\vec{\xi}_k)\prod_{a=1}^{n}\theta\left(\xi^a+\sum_k\xi_k^a+\alpha-2\right)\right]\right\},\end{aligned} \tag{10}$$

where $\xi = \sum_{a=1}^{n} \xi^a$, $\tilde{\xi} = \sum_{a=1}^{n} (\xi^a)^2$, and

$$\Lambda = \left\{ \{c(\vec{\xi}\,)\} \middle| \sum_{\vec{\xi}} c(\vec{\xi}\,) = 1, c(\vec{\xi}\,) \geqslant 0 \ (\forall \vec{\xi} \in \{\pm 1, 0\}^n) \right\}. \tag{11}$$

Introducing a Lagrange multiplier $\lambda$ for $\sum_{\vec{\xi}} c(\vec{\xi}\,) = 1$, we obtain saddle-point equations for $\{\vec{\xi}\}$ as follows:

$$c(\vec{\xi}\,) = \exp\left[ -1 + \lambda - \mu\xi + \mu^r \tilde{\xi} + c \sum_{\overrightarrow{\xi_1}, \cdots, \overrightarrow{\xi_{\alpha-1}}} \prod_{k=1}^{\alpha-1} c(\overrightarrow{\xi_k}) \prod_{a=1}^{n} \theta\left( \xi^a + \sum_{k=1}^{\alpha-1} \xi_k^a + \alpha - 2 \right) \right]. \tag{12}$$

To solve these equations, we assume the replica symmetric ansatz that the order parameter depends only on $\xi$ and $\tilde{\xi}$. Two effective fields $h_1$ and $h_2$ are then defined as

$$c(\vec{\xi}\,) \overset{\text{RS}}{=} c(\xi, \tilde{\xi}) \equiv \int dP(h_1, h_2) \frac{1}{Z^n} \exp(\mu h_1 \xi + \mu h_2 \tilde{\xi}), \tag{13}$$

where $Z = 1 + 2\exp(\mu h_2)\cosh(\mu h_1)$ [32]. Then, Eq. (12) is represented by a joint probability distribution $P(h_1, h_2)$. Using the fact that the numbers of $\xi^a = -1$ and 0 in $\vec{\xi}$ are given, respectively, by $(\tilde{\xi} - \xi)/2$ and $n - \tilde{\xi}$, we find the following:

$$\begin{aligned} \int dP(h_1, h_2) \frac{1}{Z^n} \exp(\mu h_1 \xi + \mu h_2 \tilde{\xi}) = \exp\Bigg[ & -1 + \lambda - \mu\xi + \mu^r \tilde{\xi} + c \int \prod_{k=1}^{\alpha-1} dP\left(h_1^{(k)}, h_2^{(k)}\right) \left\{ 1 - \frac{\exp\left[\mu \sum_k \left(-h_1^{(k)} + h_2^{(k)}\right)\right]}{Z^{\alpha-1}} \right\}^{n-\tilde{\xi}} \\ & \times \left( 1 - \frac{\exp\left[\mu \sum_k \left(-h_1^{(k)} + h_2^{(k)}\right)\right]}{Z^{\alpha-1}} \left\{ 1 + \sum_k \exp\left[\mu\left(h_1^{(k)} - h_2^{(k)}\right)\right] \right\} \right)^{\frac{\tilde{\xi} - \xi}{2}} \Bigg]. \end{aligned} \tag{14}$$

A Laplace transformation enables us to write down a self-consistent equation of $P(h_1, h_2)$:

$$\begin{aligned} P(h_1, h_2) = \sum_{d=0}^{\infty} e^{-c} \frac{c^d}{d!} \int \prod_{i=1}^{d} \prod_{k=1}^{\alpha-1} dP\left(h_1^{(i,k)}, h_2^{(i,k)}\right) \times \delta\left( h_1 + 1 + \sum_{i=1}^{d} u_2\left(\left\{\left(h_1^{(i,k)}, h_2^{(i,k)}\right)\right\}; \mu\right) \right) \\ \times \delta\left( h_2 - \mu^{r-1} + \sum_{i=1}^{d} \left[ u_1\left(\left\{\left(h_1^{(i,k)}, h_2^{(i,k)}\right)\right\}; \mu\right) - u_2\left(\left\{\left(h_1^{(i,k)}, h_2^{(i,k)}\right)\right\}; \mu\right) \right] \right), \end{aligned} \tag{15}$$

where

$$u_1\left(\left\{\left(h_1^{(i,k)}, h_2^{(i,k)}\right)\right\}; \mu\right) = \frac{1}{\mu} \ln\left[ 1 - \frac{\exp\left[ -\sum_{k=1}^{\alpha-1} \mu\left(h_1^{(i,k)} - h_2^{(i,k)}\right)\right]}{\prod_k \left\{ 1 + \exp\left[\mu\left(h_1^{(i,k)} + h_2^{(i,k)}\right)\right] + \exp\left[ -\mu\left(h_1^{(i,k)} - h_2^{(i,k)}\right)\right]\right\}} \right], \tag{16}$$

and

$$u_2\left(\left\{\left(h_1^{(i,k)}, h_2^{(i,k)}\right)\right\}; \mu\right) = \frac{1}{2\mu} \ln\left[ 1 - \frac{\exp\left[ -\sum_{k=1}^{\alpha-1} \mu\left(h_1^{(i,k)} - h_2^{(i,k)}\right)\right]\left(1 + \sum_k \exp\left[\mu\left(h_1^{(i,k)} - h_2^{(i,k)}\right)\right]\right)}{\prod_k \left\{ 1 + \exp\left[\mu\left(h_1^{(i,k)} + h_2^{(i,k)}\right)\right] + \exp\left[ -\mu\left(h_1^{(i,k)} - h_2^{(i,k)}\right)\right]\right\}} \right]. \tag{17}$$

Our aim is to solve this equation in the $\mu \to \infty$ limit. The parameter $r$ has a crucial role in the limit.

The following three cases are characterized by the value of $r$.

### C. Case 1: IP limit ($r > 1$)

In the case in which $r > 1$, the effective field $h_2$ diverges. Then, the self-consistent equation of $P(h_1, \infty)$ is reduced to

$$P(h_1, \infty) = \sum_{d=0}^{\infty} e^{-c} \frac{c^d}{d!} \int \prod_{i=1}^{d} dP\left(h_1^{(i)}, \infty\right) \delta\left( h_1 + 1 + 2 \sum_i \prod_{k=1}^{\alpha-1} \theta\left(-h_1^{(k)}\right) \max\left(h_1^{(1)}, \cdots, h_1^{(\alpha-1)}\right) \right). \tag{18}$$

This equation is equivalent to that of the original min-VC on $\alpha$-uniform hypergraphs [18]. $P(h_1, \infty)$ has a sharp peak around some integral values of $h_1$ if $\mu \gg 1$. We therefore assume an integer-field ansatz that the effective field $h_1$ takes an integer in the $\mu \to \infty$ limit. Equation (18) is solved under this ansatz. The average minimum cover ratio is expressed as shown below:

$$x_c^{\text{IP}}(c) = 1 - \left[ \frac{W[(\alpha-1)c]}{(\alpha-1)c} \right]^{\frac{1}{\alpha-1}} \left[ 1 + \frac{W[(\alpha-1)c]}{\alpha} \right]. \tag{19}$$

Therein, $W(x)$ denotes the Lambert's $W$ function defined by $W(x)e^{W(x)} = x$. The RS ansatz gives the correct value of $x_c^{\mathrm{IP}}(c)$ below the threshold $c^* = e/(\alpha - 1)$.

### D. Case 2: LP limit ($0 < r < 1$)

Let us consider the case in which $0 < r < 1$. Figure 2 shows a numerical solution of Eq. (15) with $\mu = 30$ obtained using the population dynamics [33]. Results show that the joint probability density $P(h_1,h_2)$ is supported on triangular parts located at $(h_1,h_2) = (m + l/2 - 1, -l/2)$ with $m,l \geqslant 0$ and $m,l \in \mathbb{Z}$. Considering that the effective fields fluctuate because of the infinitesimal penalty $\mu^{r-1}$, these values are represented by $(m + l/2 - 1 + v\mu^{r-1}, -l/2 + w\mu^{r-1})$ with some coefficients $v$ and $w$. The numerical simulations imply that the fluctuation has the following property:

$$w \geqslant 1, \quad -w + 1 \leqslant v \leqslant w - 1. \tag{20}$$

This infinitesimal-field ansatz is conserved by Eq. (15). It is also consistent with numerical solutions obtained by the population dynamics.

The joint probability distribution of the effective field is then decomposed into some probabilities with support on each triangle as

$$P(h_1,h_2) = \sum_{l,m=0}^{\infty} R(l,m) \tag{21}$$

where

$$R(l,m) = \int dP(h_1,h_2) \sum_{(v,w)\in\mathcal{D}} \delta\left[h_1 - \left(m + \frac{l}{2} - 1\right) - v\mu^{r-1}\right] \times \delta\left(h_2 + \frac{l}{2} - w\mu^{r-1}\right), \tag{22}$$

and $\mathcal{D} = \{(v,w) \in \mathbb{Z}^2 | w \geqslant 1, -w + 1 \leqslant v \leqslant w - 1\}$.

A set of effective fields $(h_1,h_2)$ is distinguished using a likelihood of spin values. We define several regions as follows: $\mathcal{P} = \{(h_1,h_2)|\, h_2 < -|h_1|\}$, $\mathcal{Q} = \{(h_1,h_2)|\, h_2 > h_1, h_1 < 0\}$, $\mathcal{R} = \{(h_1,h_2)|\, h_2 > 0, h_1 = 0\}$, and $\mathcal{S} = \{(h_1,h_2)|\, h_2 > -h_1, h_1 > 0\}$. When we define a set of probabilities that a spin takes 1, 0, and $-1$ as $(p_1,p_0,p_{-1})$, the sets in each region of $\mathcal{P}$, $\mathcal{Q}$, $\mathcal{R}$, and $\mathcal{S}$ are $(0,1,0)$, $(0,0,1)$, $(p_\alpha,0,1-p_\alpha)$ with $p_\alpha \in (0,1)$ and $(1,0,0)$, respectively. Assuming Eq. (20), the weights of these states read

$$P = \sum_{l=2}^{\infty} R(l,0), \quad Q = R(0,0) + R(1,0), \quad R = R(0,1), \quad S = \sum_{m+l\geqslant 2, m\geqslant 1} R(l,m). \tag{23}$$

Equation (15) enables us to obtain self-consistent equations as follows:

$$\begin{aligned}
P &= \sum_k e^{-c}\frac{c^k}{k!}\{1 - (Q')^{\alpha-1}\}^k - Q = e^{-c(Q')^{\alpha-1}} - Q,\\
Q &= Q' + Q'',\\
Q' &= \sum_k e^{-c}\frac{c^k}{k!}\{1 - (Q')^{\alpha-1} - (\alpha-1)(P+Q'')(Q')^{\alpha-2}\}^k\\
&= \exp[-c(Q')^{\alpha-2}\{(\alpha-1)(P+Q) - (\alpha-2)Q\}],\\
Q'' &= \sum_k e^{-k}\frac{c^k}{k!}k(\alpha-1)(P+Q'')(Q')^{\alpha-2}\\
&\quad\times\{1 - (Q')^{\alpha-1} - (\alpha-1)(P+Q'')(Q')^{\alpha-2}\}^{k-1}\\
&= c(\alpha-1)(P+Q'')(Q')^{\alpha-1},\\
R &= \sum_k e^{-c}\frac{c^k}{k!}k(Q')^{\alpha-1}\\
&\quad\times\{1 - (Q')^{\alpha-1} - (\alpha-1)(P+Q'')(Q')^{\alpha-2}\}^{k-1}\\
&= c(Q')^{\alpha},\\
S &= 1 - P - Q - R,
\end{aligned} \tag{24}$$

where $Q' = R(0,0)$ and $Q'' = R(1,0)$. Substituting $X = P + Q$ and $Y = Q'$, we find

$$X = \exp(-cY^{\alpha-1}), \quad Y = \exp\{-cY^{\alpha-2}[(\alpha-1)X - (\alpha-2)Y]\}. \tag{25}$$

The spin variable takes 1 with probability $p_\alpha$ and $-1$ otherwise if $(h_1,h_2)$ is located in region $\mathcal{R}$. It is the third ansatz to consider the probability $p_\alpha = 1/\alpha$ on $\alpha$-uniform hypergraphs. Then, using the solution of Eq. (25), the LP-relaxed average minimum cover ratio reads

$$x_c^{\mathrm{LP}}(c) = 1 - \frac{1}{2}\left[X + Y + c(\alpha-1)(X-Y)Y^{\alpha-1} + 2c\frac{\alpha-1}{\alpha}Y^{\alpha}\right], \tag{26}$$

and the average fraction of half integers is represented as

$$p_h(c) = (X - Y)[1 - c(\alpha-1)Y^{\alpha-1}]. \tag{27}$$

For any $\alpha$, $X$ is equal to $Y$ below the average degree $c^* = e/(\alpha-1)$. In this case, $X = Y = [W((\alpha-1)c)/(\alpha-1)c]^{1/(\alpha-1)}$ engenders $x_c^{\mathrm{LP}}(c) = x_c^{\mathrm{IP}}(c)$ and $p_h(c) = 0$, which suggests that the LP relaxation typically solves the problem with high accuracy. However, it is apparent that $X > Y$ leads to $p_h(c) > 0$. As presented in later sections, the LP-relaxed value is apparently below the optimal one. These facts reveal

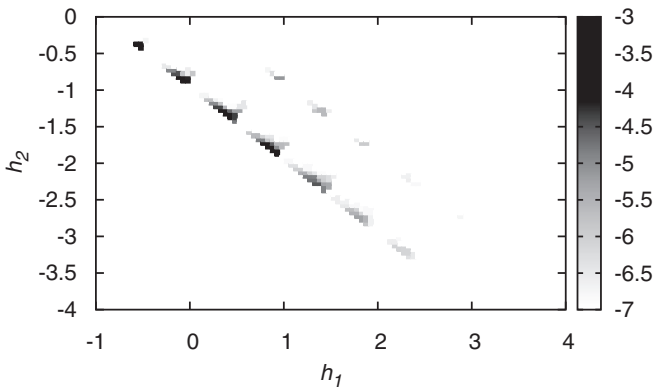


FIG. 2. Saddle-point solution $P(h_1,h_2)$ of Eq. (15) obtained using a population dynamics with $\alpha = 2$, $c = 4$, $\mu = 30$, and $r = 0.01$. The fraction on each point is shown by the logarithmic gray scale. The number of population is $10^4$ and $10^4$ iterations are executed.

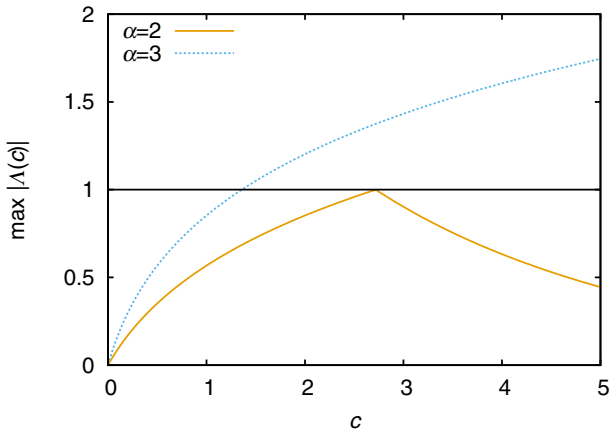


FIG. 3. Maximal absolute eigenvalue for the local-stability matrix as a function of the average degree $c$. Solid and dotted lines represent the case of min-VC ($\alpha = 2$) and min-HS ($\alpha = 3$), respectively. The horizontal solid line is $\max|\Lambda(c)| = 1$, above which the local stability breaks.

that a phase transition as for the typical behavior of the LP relaxation occurs at critical average degree $c = c^*$. In the case of $\alpha = 2$, $p_h(c)$ is equivalent to the average fraction of a core generated by a leaf removal algorithm [16] though it is not the case if $\alpha \geqslant 3$ [18].

Here, we discuss the stability of the RS solution. In terms of statistical mechanics, the convexity of the free energy called the de-Almeida and Thouless (AT) condition [34] is a reasonable qualification to study its stability. Unfortunately, however, no method has been established to verify the AT condition of the models defined on finite connectivity graphs. As a necessary condition, we study local stability of the self-consistent equations [35]. A perturbation $(\delta X, \delta Y)$ added to a possible solution $(X, Y)$ is transformed through Eq. (25) as

$$\begin{pmatrix} \delta X' \\ \delta Y' \end{pmatrix} = \begin{pmatrix} 0 & WX \\ WY & (\alpha-2)W(X-Y) \end{pmatrix} \begin{pmatrix} \delta X \\ \delta Y \end{pmatrix}, \tag{28}$$

where $W = -c(\alpha-1)Y^{\alpha-2}$. The eigenvalues of the matrix are

$$\Lambda(c) = \frac{W}{2}[(\alpha-2)(X-Y) \pm \sqrt{(\alpha-2)^2(X-Y)^2 + 4XY}]. \tag{29}$$

The solution of Eq. (15) is stable in terms of its self-consistent equations if the maximal absolute value of these eigenvalues is below 1. In the case of the min-VC with $\alpha = 2$, $\Lambda(c)$ increases below $c < c^* = e$ and reaches 1 at $c = c^*$. Above the threshold, however, it decreases and the RS solution remains stable up to $c = \infty$, as shown in Fig. 3. In contrast, $\Lambda(c)$ of min-HSs with $\alpha \geqslant 3$ increases monotonously. The RS solution loses its linear stability above the threshold. This difference shows that the half-integer relaxation in our model is insufficient for the min-HS to describe the LP-relaxed solutions, whereas the min-VC holds the half integrality.

### E. Case 3: Three-state limit

For the parameter $r < 0$, the penalty term does not affect the system. The ground states consist not only of optimal extreme-point solutions but also of other trivial ground states. The RS solution in this limit thus cannot predict the typical behavior of the LP relaxation except for its approximate value. For example, the half-integral ratio $p_h$ is always positive for any $c$, which is quite different from numerical results of the LP problem shown below.

## IV. NUMERICAL SIMULATIONS

In this section, we perform numerical simulations of two types to confirm our RS analyses in the LP limit and IP limit. One is the Markov-chain Monte Carlo simulation for estimating optimal values of the original problems. We especially use the replica-exchange Monte Carlo (EMC) [36,37] method to accelerate equilibration of the system. We set 50 replicas with different values of chemical potential. An optimal value on each graph is evaluated by the minimum density found in at least $2^{17}$ Monte Carlo steps. It is then averaged over 800 random graphs with 16–512 vertices and extrapolated to $x_c^{\mathrm{IP}}$ using a quadratic function of $N^{-1}$. The evaluated optimal values are compared to the analytical RS solutions of the LP-IP model. The other is LP relaxation. It is performed mainly to examine the validity of LP-limit solutions for both min-VCs and min-HSs. We generate at least 800 random graphs and solve the LP-relaxed problems using the LP_solve_5.5 solver. Especially in the case of min-VCs, the LR algorithm is executed as pretreatment because of accurate estimation of the half-integral ratio $p_h$.

We first discuss numerical results for the optimal or approximate values of min-VCs. Figure 4 shows optimal or approximate cover ratios obtained using the EMC and LP relaxation. For a relatively small average degree, it is apparent that the RS solutions and LP-relaxed numerical results well agree with the optimal values estimated by the EMC. This

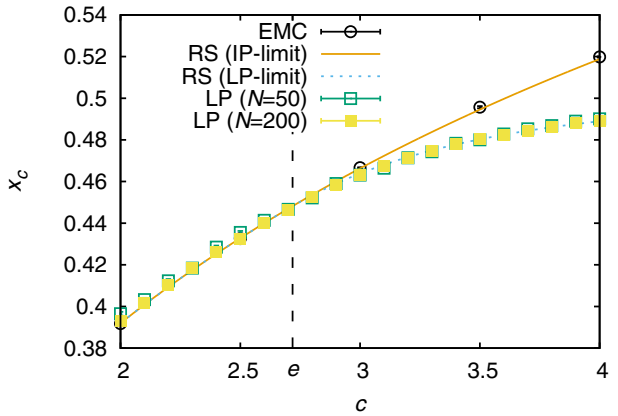


FIG. 4. The minimum-cover ratio in Erdös-Rényi random graphs with $\alpha = 2$ as a function of the average degree $c$. Circles are numerical results given by the replica exchange Monte Carlo method. Square marks are numerical results obtained using the revised simplex method with vertex cardinalities $N = 50$ (open) and 200 (filled). These are averaged over 800 random graphs for the Monte Carlo method and 1600 random graphs for the LP relaxation. The solid and dotted lines, respectively, show the RS solutions in the IP limit and the LP limit. The vertical dashed line represents the critical average degree $c^* = e$.

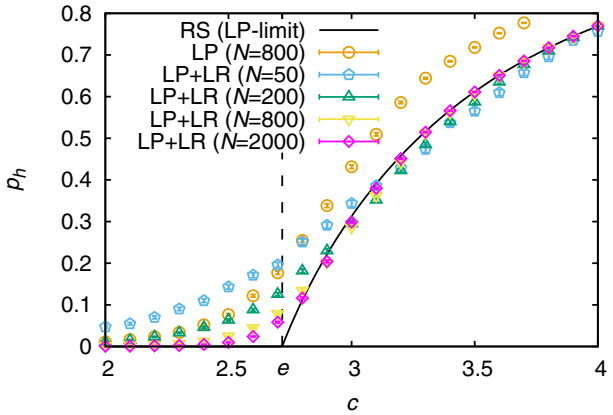


FIG. 5. Half-integral ratio $p_h$ as a function of the average degree $c$. Circles denote data obtained only using the revised simplex method with vertex cardinality $N = 800$. Other open marks are numerical results obtained using the simplex method after running a leaf removal algorithm with $N = 50$, 200, 800, and 2000. These are averaged over 1600 random graphs. The solid line represents the RS solution in the LP limit. The vertical dashed line represents the critical average degree $c^* = e$.

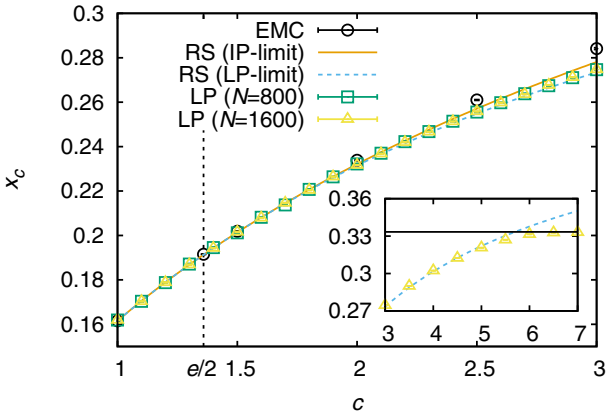


FIG. 6. Minimum-cover ratio in Erdös-Rényi random graphs with $\alpha = 3$ as a function of the average degree $c$. Circles are numerical results given by the replica exchange Monte Carlo (EMC) method. Marks denote the data obtained using the revised simplex method for vertex cardinalities of $N = 800$ (square) and 1600 (triangle). These are averaged over 800 random graphs. The solid and dotted lines, respectively, show the RS solutions in the IP limit and the LP limit. The vertical dashed line represents the critical average degree $c^* = e/2$. In the inset, the LP-relaxed approximation values obtained by numerical results with $N = 1600$ (triangle) and the RS solution in the LP limit (dashed line) are shown for relatively large $c$. The horizontal solid line is an upper bound of the LP relaxation for the min-HS ($\alpha = 3$).

shows that the LP relaxation typically approximates the original problems in good accuracy in the RS phase. In contrast, when the average degree is above the critical threshold $c = e$, the RS solutions in the IP limit become unstable. It leads to a wrong evaluation for the optimal values compared to the EMC. Then higher RSB solutions are necessary to estimate the optimal values exactly. In the case of the LP relaxation, our statistical mechanical prediction still agrees with the numerical data. We also confirm that the LP relaxation typically fails to estimate the optimal values if the average degree is larger than $c^*$. The LP-relaxed approximate value of the min-VC goes to $1/2$ in the large-$c$ limit, while the optimal value of the min-VC is asymptotically close to 1.

Next, we specifically examine the half-integral ratio $p_h$ representing a typical property of the approximate solutions. In Fig. 5, it is apparent that numerical data obtained using the LP relaxation are well above our analytic prediction. Generally speaking, LP-relaxed problems have several optimal extreme-point solutions because of the existence of a leaf, a pair of vertices both of which are of degree 1. For instance, we assume that a graph $G_2$ consists of an odd cycle and a leaf, and that a vertex in the cycle is connected to one in the leaf by an edge. Then, an LP-relaxed min-VC on $G_2$ has two solutions: one has all half-integral variables; the other has integral variables in the leaf. If one simply runs a solver, then one obtains the average ratio with half-integral variables, not the minimum ratio $p_h$ predicted by the LP-IP model. For this reason, the discrepancy in $p_h$ arises. We therefore perform an LR algorithm before executing the LP relaxation, by which half-integral variables induced by the leafs can be avoided. Figure 5 shows the minimum half-integral ratio estimated using the procedure. As expected, the modified LP method reduces the number of half-integral variables after performing the LR algorithm. Therefore, this LR+LP method obtains the optimal extreme-point solutions and improves the numerical estimation of $p_h$. Although there remains a finite-size effect for small sizes and around the threshold $c \simeq e$, the numerical estimations are close to the analytic results with increasing size. Our analysis correctly predicts not only the approximate value of $x_c$ but also the typical property of the LP relaxation.

Lastly, we present the case of min-HS problems with $\alpha = 3$. Figure 6 shows the optimal values estimated using the EMC and the approximate values obtained by the LP relaxation, together with the analytical results derived in the previous section.

All the results coincide mutually for a sufficiently small average degree. The relaxed values, however, are markedly smaller than the optimal values of the original problem above the critical average degree $c = e/2$, where the replica symmetry of the min-HS is broken. We therefore confirm that the LP relaxation typically fails to approximate min-HSs in the RSB region. As a striking difference between min-VCs and min-HSs, we point out that the RS solutions in the LP limit are also unstable above the critical threshold. Whereas the discrepancy between the numerical LP-relaxed results and the analytic estimations is quite small as shown in Fig. 6, it increases gradually as $c$ becomes large as one can see in its inset.

In the large-$c$ limit, the LP-relaxed value on $\alpha$-uniform graphs converges to $1/\alpha$ whereas the analytic solutions converge to $1/2$. Our result implies that the existence of the RSB region in the LP limit results from the lack of half integrality in min-HSs. To obtain a better analytic prediction, one must consider the model with more degrees of freedom, beyond the half-integrality condition.

## V. SUMMARY AND DISCUSSION

In this paper, we describe the details of the statistical mechanical analysis of typical behavior of the LP relaxation.

The LP relaxation of the min-VC can be mapped onto the LP-IP model with three-state Ising variables assisted by the novel property called half integrality. Three distinct ground states are derived by fixing a parameter $r$ of the model and taking a large field (zero temperature) limit. The replica method in the spin-glass theory enables us to solve the model approximately in these limits. In the IP limit with $r > 1$, the ground states are reduced to optimal solutions of the original min-VCs. The ground states in the LP limit with $0 < r < 1$ correspond to the LP-relaxed approximate solutions with minimum half-integral variables. In the three-state limit with $r < 0$, the ground states are not constructed by the extreme-point solutions which are unsuitable for the LP-relaxed solution. The RS solution in the LP limit is stable for the arbitrary average degree. Therefore, the LP-limit solution coincides with the numerical result. However, the RS solution in the IP limit is unstable above $c^* = e$. In fact the LP relaxation fails to approximate optimal solutions above the critical threshold.

We also discuss the case of the min-HS, min-VCs on $\alpha$-uniform hypergraphs. Because the min-HS has no half integrality, the LP-IP model with three-state Ising is insufficient for describing the LP relaxation of the min-HS. It is, however, worth studying the LP-IP model for a half-integer relaxed problem toward an understanding of the LP relaxation.

It is particularly interesting that the RS solution in the LP limit is still stable below the critical threshold of the min-HS. This stability suggests that the original problem is stable against addition of the half-integral variables to its solution. Above the threshold, the analytic estimation by the RS solution in the LP limit deviates from the optimal value of the original problem. The RS solution is simultaneously unstable, meaning the emergence of the RSB solutions. This fact implies that the half-integer relaxed problem decreases the value of the cost function from the original problem but it is still typically difficult to solve. In fact, LP-relaxed approximate solutions obtained using the numerical simulations include not only half integers but also other real values. These results suggest that the LP-relaxed min-HS typically fails to approximate the original problem in the RSB region.

One of the striking facts obtained through our analysis is that, in the case of $\alpha = 2$, the minimum half-integral ratio $p_h$ has the same mathematical expression as the LR core [16]. It strongly suggests that a common graph structure is the origin of the wrong estimation in two different approximation algorithms, which is unfortunately not identified. A key ingredient of the graph structure may be the core, in which there exist entangled odd long cycles and clustering of the optimal solutions occurs [38]. In min-$K$-XORSAT, a $K$ core is also regarded as a trigger for the typical hardness [39]. Then, it is naively expected that some graph structures will be a cause of both the replica symmetry breaking and the typical hardness in other combinatorial optimization problems. As for min-HSs, in contrast, it is an open problem whether the minimum nonintegral ratio is related to the core ratio. In general, the relation between an emergence of some graph structures and the RS-RSB transition is thus still to be revealed. It is interesting to consider the RSB picture more generally from the perspective of graph topology.

In this paper, we utilize the half integrality for constructing the LP-IP model. Recently, from the view of discrete convexity, bisubmodular relaxation which is equivalent to the LP relaxation with half integrality is proposed [40]. It is related closely to an approximation technique previously known as the roof duality. It has been applied to more general approximation called generalized roof duality in optimization and inference [41]. Because variables in a relaxed problem take $\{0, 1/2, 1\}$, the LP-IP model and its analyses in this paper are applicable to the relaxation. Statistical mechanical approaches will be of help to elucidate a typical property of these schemes theoretically.

We have demonstrated statistical mechanical analysis of the typical behavior of an approximation algorithm for combinatorial optimization problems. Particularly, we emphasize the LP relaxation based on the simplex method, which searches extreme points of a polytope generated by constraints. We construct the effective model as the LP-IP model by extending the degree of freedom of spins and adding a penalty term to a conventional hard-core lattice-gas model for the min-VC. Within the framework of the LP relaxation, the theoretical standard model is necessary for the relaxed problems without the half integrality and also for other solvers such as a cutting-plane approach [42]. Another task is a statistical mechanical study on other relaxations proposed in the literature of mathematical optimization. These analyses are expected to be helpful to provide conjectures related to the average complexity of optimization problems in theoretical computer science and probability theory. We hope that they are useful to investigate the deep relation between the spin-glass theory and optimization problems.

## ACKNOWLEDGMENTS

This research was supported by Grants-in-Aid for Scientific Research from Ministry of Education, Culture, Sports, Science and Technology, Japan (Grants No. 22340109, No. 25610102, and No. 25120010); for Japan Society for the Promotion of Science (JSPS) fellows (Grant No. 15J09001); and by the JSPS Core-to-Core program "Non-equilibrium dynamics of soft-matter and information."

## APPENDIX: CAVITY ANALYSIS OF THE LP-IP MODEL

In this Appendix, we present detailed analyses of the model discussed in this paper using the alternative cavity method. Although we explain the case of $\alpha$-uniform random hypergraphs here, it is straightforward to calculate more general models defined on a sparse hypergraph.

Using a factor graph representation $G = (V, F, E)$, the LP-IP model (6) is represented as

$$\Xi_r(G) = \sum_{\boldsymbol{\sigma}} \exp\left(-\mu \sum_i \sigma_i - \mu^r \sum_i \left(1 - \sigma_i^2\right)\right) \prod_{a \in F} \theta\left(\sum_{j \in \partial a} \sigma_j + \alpha - 2\right), \tag{A1}$$

where $\partial a = \{i \in V \mid (a,i) \in E\}$. We assume that the graph is locally treelike and that it has no degree correlations. By the Bethe-Peierls (BP) approximation, the likelihood that a variable on vertex $i$ takes $\sigma$ is

$$P_i(\sigma) \simeq \frac{1}{Z_i} \exp(-\mu\sigma - \mu^r \delta_{\sigma,0}) \prod_{a \in \partial i} P_{a\backslash i}(\sigma), \tag{A2}$$

where $P_{a\backslash i}(\sigma)$ is the marginal probability of $\boldsymbol{\sigma}_{\partial a\backslash i}$ under the condition $\sigma_i = \sigma$. We similarly define $P_{i\backslash a}(\sigma)$ as a probability of $\sigma_i = \sigma$ on a cavity graph $G\backslash a$. These probabilities are regarded as messages on the graph. They satisfy the following recursive relations:

$$P_{i\backslash a}(\sigma) \simeq \frac{1}{Z_{i\to a}} \exp(-\mu\sigma - \mu^r \delta_{\sigma,0}) \prod_{b \in \partial i\backslash a} P_{b\backslash i}(\sigma), \tag{A3}$$

$$P_{a\backslash i}(\sigma) \simeq \frac{1}{Z_{a\to i}} \sum_{\boldsymbol{\sigma}_{\partial a\backslash i}} \theta\left(\sigma + \sum_{j \in \partial a\backslash i} \sigma_j + \alpha - 2\right) \prod_{j \in \partial a\backslash i} P_{j\backslash a}(\sigma_j). \tag{A4}$$

By substituting a spin value, we obtain

$$\begin{aligned} P_{i\backslash a}(1) &\simeq \frac{1}{Z_{i\to a}} e^{-\mu} \prod_{b \in \partial i\backslash a} P_{b\backslash i}(1), \\ P_{i\backslash a}(0) &\simeq \frac{1}{Z_{i\to a}} e^{-\mu^r} \prod_{b \in \partial i\backslash a} P_{b\backslash i}(0), \\ P_{i\backslash a}(-1) &\simeq \frac{1}{Z_{i\to a}} e^{\mu} \prod_{b \in \partial i\backslash a} P_{b\backslash i}(-1), \end{aligned} \tag{A5}$$

and

$$\begin{aligned} P_{a\backslash i}(1) &\simeq \frac{1}{Z_{a\to i}}, \\ P_{a\backslash i}(0) &\simeq \frac{1}{Z_{a\to i}} \left(1 - \prod_{j \in \partial a\backslash i} P_{j\backslash a}(-1)\right), \\ P_{a\backslash i}(-1) &\simeq \frac{1}{Z_{a\to i}} \left(1 - \prod_{j \in \partial a\backslash i} P_{j\backslash a}(-1) - \sum_{k \in \partial a\backslash i} P_{k\backslash a}(0) \prod_{j \in \partial a\backslash \{i,k\}} P_{j\backslash a}(-1)\right). \end{aligned} \tag{A6}$$

It is convenient to introduce cavity fields defined as shown below:

$$\begin{aligned} P_{i\backslash a}(\sigma) &\equiv \frac{e^{\mu\xi_{i\to a}\delta(\sigma,1) + \mu\nu_{i\to a}\delta(\sigma,0)}}{1 + e^{\mu\xi_{i\to a}} + e^{\mu\nu_{i\to a}}}, \\ P_{a\backslash i}(\sigma) &\equiv \frac{e^{\mu\hat{\xi}_{a\to i}\delta(\sigma,1) + \mu\hat{\nu}_{a\to i}\delta(\sigma,0)}}{1 + e^{\mu\hat{\xi}_{a\to i}} + e^{\mu\hat{\nu}_{a\to i}}}, \end{aligned} \tag{A7}$$

where $\delta(\cdot,\cdot)$ is Kronecker's delta. BP equations for these fields are explicitly written down as

$$\begin{aligned} \xi_{i\to a} &= -2 + \sum_{b \in \partial i\backslash a} \hat{\xi}_{b\to i}, \quad \nu_{i\to a} = -1 - \mu^{r-1} + \sum_{b \in \partial i\backslash a} \hat{\nu}_{b\to i}, \quad \hat{\xi}_{a\to i} = \frac{1}{\mu} \\ &\quad \times \ln\left[1 - \left(1 + \sum_{k \in \partial a\backslash i} e^{\mu\nu_{k\to a}}\right) \prod_{j \in \partial a\backslash i} \frac{1}{1 + e^{\mu\xi_{j\to a}} + e^{\mu\nu_{j\to a}}}\right], \\ \hat{\nu}_{a\to i} &= \frac{1}{\mu} \ln\left[1 - \prod_{j \in \partial a\backslash i} \frac{1}{1 + e^{\mu\xi_{j\to a}} + e^{\mu\nu_{j\to a}}}\right] - \frac{1}{\mu} \ln\left[1 - \left(1 + \sum_{k \in \partial a\backslash i} e^{\mu\nu_{k\to a}}\right) \prod_{j \in \partial a\backslash i} \frac{1}{1 + e^{\mu\xi_{j\to a}} + e^{\mu\nu_{j\to a}}}\right]. \end{aligned} \tag{A8}$$

Here, we consider a graph ensemble for which the degree distribution of variable nodes is $p_k$ ($k \geqslant 0$). Letting $\tilde{P}(\xi,\nu)$ be a frequency distribution of a set of cavity fields $(\xi,\nu)$, then from Eq. (A8) we find a self-consistent equation of $\tilde{P}(\xi,\nu)$ as

$$\tilde{P}(\xi,\nu) = \sum_{k=0}^{\infty} \frac{kp_k}{c} \int \prod_{i=1}^{k-1} \prod_{j=1}^{\alpha-1} d\tilde{P}(\xi^{(i,j)},\nu^{(i,j)}) \delta\left(\xi + 2 + \sum_{i=1}^{k-1} v_2(\{\xi^{(i,j)}\},\{\nu^{(i,j)}\};\mu)\right) \times \delta\left(\nu + 1 + \mu^{r-1} - \sum_{i=1}^{k-1} [v_1(\{\xi^{(i,j)}\},\{\nu^{(i,j)}\};\mu) - v_2(\{\xi^{(i,j)}\},\{\nu^{(i,j)}\};\mu)]\right), \tag{A9}$$

where

$$v_1(\{\xi^{(i,j)}\},\{\nu^{(i,j)}\};\mu) = \frac{1}{\mu} \ln \left[1 - \prod_{j=1}^{\alpha-1} \frac{1}{1 + e^{\mu\xi^{(i,j)}} + e^{\mu\nu^{(i,j)}}}\right], \tag{A10}$$

and

$$v_2(\{\xi^{(i,j)}\},\{\nu^{(i,j)}\};\mu) = \frac{1}{\mu} \ln \left[1 - \left(1 + \sum_j e^{\mu\nu^{(i,j)}}\right) \prod_{j=1}^{\alpha-1} \frac{1}{1 + e^{\mu\xi^{(i,j)}} + e^{\mu\nu^{(i,j)}}}\right]. \tag{A11}$$

To obtain the single-spin probability $P_i(\sigma)$, we also introduce effective fields such as cavity fields and obtain the frequency distribution of those fields. In the case of Erdös-Rényi random graphs, the distribution is equivalent to that of cavity fields because an identity $p_{k-1} = kp_k/c$ ($k \geqslant 1$) holds.

By interpreting the definition of effective fields appropriately, it is apparent that the self-consistent equation is equivalent to Eq. (15) obtained using the replica method. Further assumptions are necessary to analyze the case of the large-$\mu$ limit. They correspond to the ansatz discussed in Sec. III D. We correctly obtain the typical property of the LP relaxation by taking the LP limit.


[1] L. G. Khachiyan, Zh. Vychisl. Mat. Mat. Fiz. **20**, 53 (1980).
[2] M. Desrochers, J. Desrosiers, and M. Solomon, Oper. Res. **40**, 342 (1992).
[3] K. Hoffman and M. Padberg, Management Science **39**, 657 (1993).
[4] D. Malioutov and M. Malyutov, in *Proceedings of the IEEE International Conference on Acoustics, Speech and Signal Processing (ICASSP)* (IEEE Signal Processing Society, Piscataway, 2012), p. 3305.
[5] V. V. Vazirani, *Approximation Algorithms* (Springer, Berlin, 2004).
[6] A. Frieze and C. McDiarmid, Random Struct. Alg. **10**, 5 (1997).
[7] M. Mézard, G. Parisi, and M. Á. Virasoro, *Spin Glass Theory and Beyond* (World Scientific, Singapore, 1987), p. 5.
[8] Y. Fu and P. W. Anderson, J. Phys. A **19**, 1605 (1986).
[9] R. Monasson, R. Zecchina, S. Kirkpatrick, B. Selman, and L. Troyansky, Nature (London) **400**, 133 (1999).
[10] R. M. Karp and M. Sipser, in *Proceedings of the 22nd Annual Symposium on Foundations of Computer Science* (IEEE Computer Society, Los Alamitos, 1981), p. 364.
[11] S. Khot and O. Regev, J. Comp. System Sci. **74**, 335 (2008).
[12] A. K. Hartmann and M. Weigt, *Phase Transitions in Combinatorial Optimization Problems* (Wiley-VCH, Weinheim, 2005).
[13] M. Weigt and A. K. Hartmann, Phys. Rev. Lett. **84**, 6118 (2000).
[14] H. Zhou, Eur. Phys. J. B **32**, 265 (2003).
[15] M. Mézard and M. Tarzia, Phys. Rev. E **76**, 041124 (2007).
[16] M. Bauer and O. Golinelli, Eur. Phys. J. B **24**, 339 (2001).
[17] M. Weigt, Eur. Phys. J. B **28**, 369 (2002).
[18] S. Takabe and K. Hukushima, Phys. Rev. E **89**, 062139 (2014).
[19] C. Lucibello and F. Ricci-Tersenghi, Int. J. Stat. Mech. (2014) 136829.
[20] J. Inoue, J. Phys. A **30**, 1047 (1997).
[21] F. F. Ferreira and J. F. Fontanari, Physica A **269**, 54 (1999).
[22] S. Sanghavi and D. Shah, arXiv:cs/0508097 (2005).
[23] T. Dewenter and A. K. Hartmann, Phys. Rev. E **86**, 041128 (2012).
[24] S. Takabe and K. Hukushima, J. Phys. Soc. Jpn. **83**, 043801 (2014).
[25] A. J. Hoffman and J. B. Kruskal, in *Linear Inequalities and Related Systems*, edited by H. W. Kuhn and A. J. Tucker (Princeton University, Princeton, NJ, 1956), p. 223.
[26] M. Mézard and A. Montanari, *Information, Physics, and Computation* (Oxford University, Oxford, 2009), p. 429.
[27] M. Weigt and H. Zhou, Phys. Rev. E **74**, 046110 (2006).
[28] G. B. Dantzig, in *The Basic George B. Dantzig* (Stanford University, Stanford, 2003), p. 19.
[29] G. L. Nemhauser and L. E. Trotter Jr., Math. Program. **6**, 48 (1974).
[30] M. Berkelaar, K. Eikland, and P. Notebaert, http://lpsolve.sourceforge.net/5.5/.
[31] R. Monasson, J. Phys. A **31**, 513 (1998).
[32] R. Erichsen Jr. and W. K. Theumann, Phys. Rev. E **83**, 061126 (2011).
[33] M. Mezard and G. Prisi, Eur. Phys. J. B **20**, 217 (2001).
[34] J. R. L. de Almeida and D. J. Thouless, J. Phys. A **11**, 983 (1978).
[35] L. Zdeborova and M. Mézard, J. Stat. Mech. (2006) P05003.
[36] C. J. Geyer, in *Computing Science and Statistics: Proceedings of the 23rd Symposium on the Interface*, edited by E. M. Keramidas (Interface Foundation of North America, Fairfax Station, 1991), p. 156.

[37] K. Hukushima and K. Nemoto, J. Phys. Soc. Jpn. **65**, 1604 (1996).
[38] W. Barthel and A. K. Hartmann, Phys. Rev. E **70**, 066120 (2004).
[39] M. Mézard, F. Ricci-Tersenghi, and R. Zecchina, J. Stat. Phys. **111**, 505 (2003).
[40] V. Kolmogorov, Discrete Appl. Math. **160**, 416 (2012).
[41] F. Kahl and P. Strandmark, Discrete Appl. Math. **160**, 2419 (2012).
[42] A. Schrijver, *Theory of Linear and Integer Programming* (Wiley, West Sussex, 1986), p. 339.